www.nature.com/cdd

CDDpress

ARTICLE

The E3 ubiquitin ligase TRIM31 plays a critical role in hypertensive nephropathy by promoting proteasomal degradation of MAP3K7 in the TGF-β1 signaling pathway

Jie Zhang[1], Lei Cao[1], Xiaohong Wang[1], Qian Li[1], Meng Zhang[1], Cheng Cheng[1], Liwen Yu[1], Fei Xue[1], Wenhai Sui[1], Shangwen Sun[1], Na li[1], Peili Bu[1], Bingyu Liu[2], Fei Gao[1], Junhui Zhen[3], Guohai Su[4], Cheng Zhang[1,4], Chengjiang Gao[2✉], Meng Zhang[1,4✉] and Yun Zhang[1,4✉]

Renal fibrosis and inflammation are critical for the initiation and progression of hypertensive renal disease (HRD). However, the signaling mechanisms underlying their induction are poorly understood, and the role of tripartite motif-containing protein 31 (TRIM31), an E3 ubiquitin ligase, in HRD remains unclear. This study aimed to elucidate the role of TRIM31 in the pathogenesis of HRD, discover targets of TRIM31, and explore the underlying mechanisms. Pathological specimens of human HRD kidney were collected and an angiotensin II (AngII)-induced HRD mouse model was developed. We found that TRIM31 was markedly reduced in both human and mouse HRD renal tissues. A TRIM31$^{-/-}$ mice was thus constructed and showed significantly aggravated hypertension-induced renal dysfunction, fibrosis, and inflammation, following chronic AngII infusion compared with TRIM31$^{+/+}$ mice. In contrast, overexpression of TRIM31 by injecting adeno-associated virus (AAV) 9 into C57BL/6J mice markedly ameliorated renal dysfunction, fibrotic and inflammatory response in AngII-induced HRD relative to AAV-control mice. Mechanistically, TRIM31 interacted with and catalyzed the K48-linked polyubiquitination of lysine 72 on Mitogen-activated protein kinase kinase kinase 7 (MAP3K7), followed by the proteasomal degradation of MAP3K7, which further negatively regulated TGF-β1-mediated Smad and MAPK/NF-κB signaling pathways. In conclusion, this study has demonstrated for the first time that TRIM31 serves as an important regulator in AngII-induced HRD by promoting MAP3K7 K48-linked polyubiquitination and inhibiting the TGF-β1 signaling pathway.

Cell Death & Differentiation (2022) 29:556–567; https://doi.org/10.1038/s41418-021-00874-0

INTRODUCTION

Hypertension, a major risk factor for cardiovascular and cerebrovascular diseases, is closely related to the occurrence and development of chronic kidney disease [1, 2], Angiotensin II (AngII), the major effector of the renin-angiotensin system, is a key mediator in the progression of hypertensive nephropathy (HRD) [3, 4]. The kidneys are one of the prime targets of chronic hypertension-related injury, which manifests primarily as proteinuria [5], renal interstitial fibrosis with excessive deposition of extracellular matrix proteins such as collagens and fibronectin [6, 7], chronic inflammation accompanied by increased expression of tumor necrosis factor α (TNF-α), interleukin 6 (IL-6) and interleukin 1β (IL-1β) [8], and vascular remodeling [9, 10]. Variety of cells were involved in the process of chronic kidney injury, such as tubular epithelial cells, fibroblasts, podocytes, inflammatory cells, vascular endothelial cells, pericytes and so on [11–16]. However, the pathogenesis of HRD has not been fully elucidated.

Transforming growth factor-β (TGF-β)1, which could be induced by AngII, has been reported to play a predominant role in the process of hypertensive renal fibrosis [6]. It accelerates progressive renal fibrosis by promoting extracellular matrix production while inhibiting its degradation, and regulating the inflammatory response by stimulating the expression of various cytokines [17]. It also induces de-differentiation of epithelial and endothelial cells [18–21]. TGF-β1 mediates renal fibrosis by regulating canonical Smad-dependent (involving phosphorylation and activation of Smad2 and Smad3) [22] and non-canonical Smad-independent signaling, in particular, the TRAF6-MAP3K7-MAPK/NF-κB pathway [17]. Mitogen-activated protein kinase kinase kinase 7 (MAP3K7), could be activated by TGF-β1, which further act as an upstream activator of the MKK/JNK signal transduction cascade and the p38 MAPK signal transduction cascade through the phosphorylation and activation of several MAP kinase kinases. It is regulated by various cytokines and functions in TGF-β1-mediated MAPK and NF-κB

[1]The Key Laboratory of Cardiovascular Remodeling and Function Research, Chinese Ministry of Education, Chinese National Health Commission and Chinese Academy of Medical Sciences, The State and Shandong Province Joint Key Laboratory of Translational Cardiovascular Medicine, Department of Cardiology, Qilu Hospital, Cheeloo College of Medicine, Shandong University, Jinan, China. [2]Shandong Key Laboratory of Infection and Immunity, Department of Immunology, School of Basic Medical Sciences, Shandong University, Jinan, China. [3]Department of Pathology, Qilu Hospital of Shandong University, Jinan, China. [4]Cardiovascular Disease Research Center of Shandong First Medical University, Central Hospital Affiliated to Shandong First Medical University, Jinan, China. ✉email: cgao@sdu.edu.cn; zhangmeng@sdu.edu.cn; zhangyun@sdu.edu.cn

Edited by V D'Angiolella

Received: 28 February 2021 Revised: 10 September 2021 Accepted: 13 September 2021
Published online: 28 September 2021

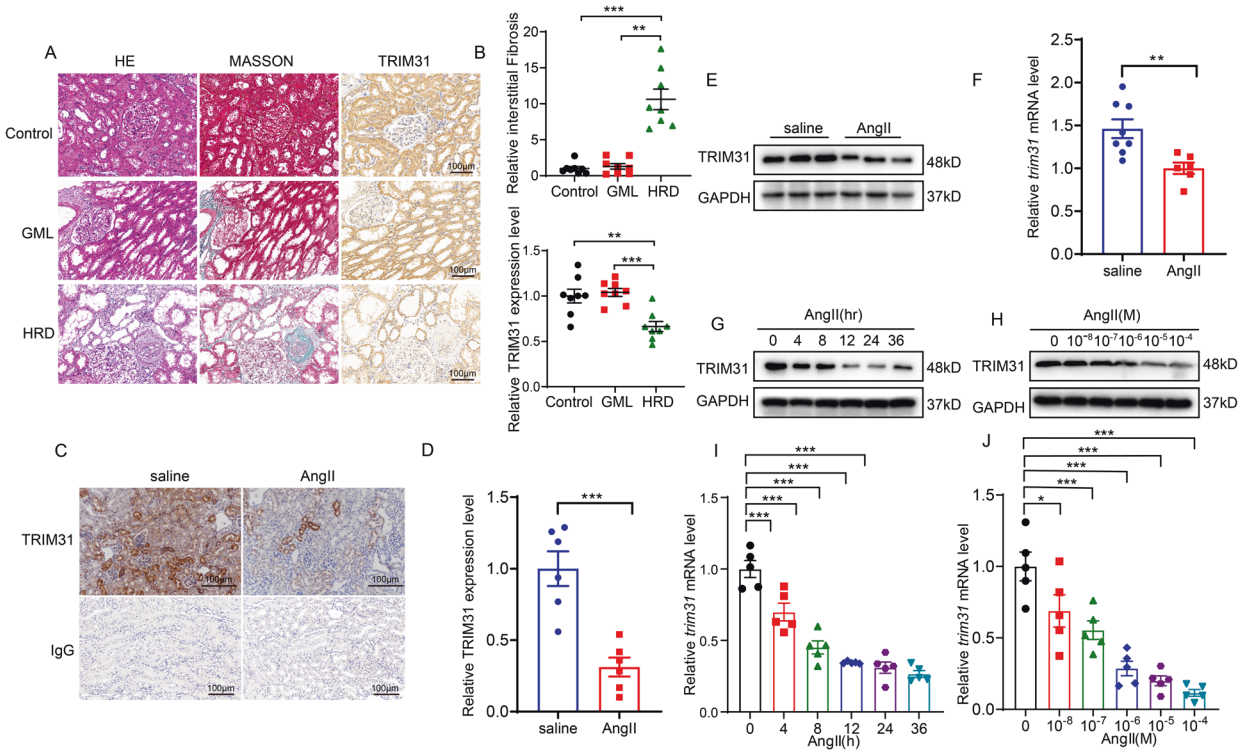

Fig. 1 TRIM31 levels were significantly reduced in human and mouse hypertensive kidneys. A Representative photographs of H&E, Masson, and IHC staining of TRIM31 in Control, GML, and HRD human kidney specimens. **B** Quantitation of Masson and IHC staining of TRIM31 in Control, GML, and HRD human kidney specimens. $n = 8$ per group. **C**, **D** Representative IHC staining images and quantitation of TRIM31 in the kidney after saline or AngII treatment in WT mice. $n = 6$ per group. **E** Immunoblot assay of TRIM31 expression in kidneys after saline or AngII treatment in WT mice. GAPDH was used for normalization. **F** Relative mRNA levels of *trim31* expression in kidneys after saline ($n = 8$) or AngII treatment ($n = 6$) in WT mice. **G**, **H** Representative Western blot images of TRIM31 in HK2 cells after AngII stimulation at a concentration of 10^{-6} M for different period of time, or at different concentrations for 24 h. **I**, **J** Relative *trim31* mRNA levels in HK2 cells after AngII stimulation at a concentration of 10^{-6} M for indicated periods of time, or at indicated concentrations for 24 h. $n = 5$ per group. Data were presented as mean ± SEM and normal distributions were tested by Shapiro–Wilk method, which showed that all the data except those in **B** (Relative interstitial fibrosis) were normally distributed. One-way ANOVA with Dunnett post hoc test was used for **B** (Relative TRIM31 expression level), **I** and **J**. * adjusted $P < 0.05$, ** adjusted $P < 0.01$, *** adjusted $P < 0.001$. Kruskal–Wallis test with Dunnett post hoc tests was used for **B** (Relative interstitial fibrosis). Adjusted P values were provided in case of multiple groups comparisons. Student's t test was used for **D** and **F**. *$P < 0.05$, **$P < 0.01$, ***$P < 0.001$. Each experiment was repeated independently for a minimum three times.

activation [23, 24]. It is involved in various pathophysiological processes, including cardiac hypertrophy and fibrosis, inflammation, and apoptosis [25]. However, the role of MAP3K7 in Smad-dependent pathways is controversial [26]. Further, the molecular mechanism by which TGF-β1 contributes to HRD, and the roles of MAP3K7 in Smad-dependent and -independent pathways remain elusive and merit exploration.

The tripartite motif (TRIM) family of proteins is an evolutionarily conserved E3 ubiquitin ligase family. TRIM proteins contain an interesting new gene (Ring) domain conferring E3 ubiquitin ligase activity, one or two B-box motifs, and a coiled-coil (C-C) region [27]. Accumulating evidence indicates that dysregulation of TRIM proteins causes several disorders, including immune diseases [28], cancer, hepatic fibrosis, and inflammation [29], by promoting lysine (K) 6, K11, K27, K29, K33, K48, and K63-linked covalent polyubiquitination of proteins [30]. Moreover, TRIM31 exhibits autoubiquitination activity. Early studies indicated that TRIM31 plays a key role in a broad range of biological events, particularly, in the innate immune response [31], NLRP3 inflammasome activation [32], intestinal microbiota composition [33], and intestinal autophagy [34, 35]. However, whether it plays a role in HRD and its specific mechanism remain unclear.

Polyubiquitination of MAP3K7 is a non-canonical pathway activated by TGF-β1 [36]. Several TRIM proteins can ubiquitinate MAP3K7 [37, 38]. K63-linked polyubiquitination of MAP3K7 at Lys158 is essential for its own kinase activation and its ability to mediate downstream signaling in response to TNF-α and IL-1β stimulation [39]. Only one E3 ligase, Itch, targets MAP3K7 for K48-linked ubiquitination to terminate inflammatory tumor necrosis factor signaling, but the specific lysine modification sites were not indentified [38, 40]. Previous studies have also shown that Lys(K) 72 of MAP3K7 can undergo K48-linked ubiquitination by unidentified E3 ligase and this modification on doxorubicin or TNFα -induced inflammatory responses [41, 42]. Until now, The E3 ligase that modified MAP3K7 for K48 ubiquitination, especially in TGF-β1 signaling pathway, has not been reported.

In summary, whether TRIM31 is involved in hypertensive nephropathy and the specific mechanism regulating this involvement have not been reported, and the mechanism of K48-linked ubiquitination of MAP3K7 in TGF-β1 signaling is unclear. In this study, we found that TRIM31 is closely related to renal fibrosis and inflammation in AngII-induced hypertensive mice and in human renal tubular epithelial cells. Surprisingly, TRIM31 could catalyze K48 ubiquitination and proteasomal degradation of MAP3K7 via ubiquitination on K72, which in turn affected the inflammatory and fibrosis response in HRD model mice. Moreover, human kidney specimens of HRD were collected to demonstrate the association between TRIM31 and HRD.

MATERIALS AND METHODS

A detailed method is available in the Online Supplemental Materials.

RESULTS

TRIM31 levels were significantly reduced in human and mouse HRD

To investigate the role of TRIM31 in hypertension-mediated kidney injury, we collected human renal cortical tissues from the poles of healthy kidneys of individuals ($n = 8$, each group) who underwent tumor nephrectomy without kidney disease (Control), patients with glomerular minor lesion (GML), and patients with HRD. Hematoxylin and eosin (H&E) and Masson stained sections revealed pathological changes in the GML and HRD groups, and TRIM31 expression was significantly reduced in HRD sections (Fig. 1A, B). We established a mouse model of HRD by AngII infusion for 42 days. IHC (Fig. 1C, D) showed that TRIM31 was expressed in both glomeruli and renal tubules, and its expression was significantly decreased in the condition of HRD, especially in tubules. Western blot (Fig. 1E) and RT-PCR (Fig. 1F) also revealed a decrease in TRIM31 expression. As the functional basis of renal tubules, tubular epithelial cells mediate both inflammatory response and fibrosis, and play a key role in HRD. In cultured human proximal renal tubular epithelial cells (HK2) stimulated with various concentrations of AngII, TRIM31 protein (Fig. 1G, H) and mRNA levels (Fig. 1I, J) decreased in a time- and concentration-dependent manner. These results indicated that TRIM31 may be involved in the function of renal tubular epithelial cells and the development of HRD.

TRIM31 deficiency aggravated AngII-induced kidney injury

To investigate the physiological role of TRIM31 in HRD, we generated TRIM31$^{-/-}$ mice using transcription activator-like effector nuclease technology. Effective knockout was confirmed by sequencing analysis of tail genomic DNA from TRIM31$^{+/+}$ and TRIM31$^{-/-}$ mice (Fig. 2A) and Western blot analysis of kidney tissues (Fig. 2B). TRIM31$^{+/+}$ and TRIM31$^{-/-}$ mice received AngII infusion to induce HRD or saline as a control treatment via osmotic minipumps [43] for 6 weeks. Radiotelemetry (Data Sciences International) was applied to detect mouse blood pressure changes. Both systolic and diastolic blood pressures showed a gradual increase in mice receiving AngII infusion, which reached the diagnostic standard of hypertension [44] (systolic blood pressure (SBP)/diastolic blood pressure (DBP): 141.2 ± 1.45/111 ± 2.8 mm Hg in TRIM31$^{+/+}$ mice, and 137.8 ± 1.03/105 ± 2.07 mm Hg in TRIM31$^{-/-}$ mice) one week after AngII infusion, and were significantly higher than that in saline-treated mice (SBP/DBP: 118.6 ± 2.75/86.01 ± 3.74 mmHg in TRIM31$^{+/+}$ mice, 121.1 ± 1.52/88.52 ± 2.20 mmHg in TRIM31$^{-/-}$ mouse). However, neither SBP nor DBP showed significant difference between TRIM31$^{+/+}$ and TRIM31$^{-/-}$ mouse groups after AngII or saline infusion (Fig. 2C). At the end of the experiment, the kidney-to-body-weight ratio was similar in TRIM31$^{+/+}$ and TRIM31$^{-/-}$ mice receiving AngII or saline infusion (Supplementary Fig. S1A, B). Blood urea nitrogen (BUN), serum creatinine (Cr), serum uric acid (UA), and 24-h urine albumin contents were elevated after AngII infusion. BUN and serum Cr were significantly higher in TRIM31$^{-/-}$ mice than in TRIM31$^{+/+}$ AngII-treated mice (Fig. 2D). Western blot and IHC showed that the kidney levels of nephrin, a structural protein that may be suppressed in injured podocytes, were decreased after AngII treatment, especially in TRIM31$^{-/-}$ mice (Fig. 2E, F). Meanwhile, Kidney Injury Molecule 1 (Kim-1), as one of the functional indicators of renal tubular injury, was significantly increased in Western blot, PCR and IHC staining after pumping AngII, and was more expressed in hypertensive kidneys of TRIM31$^{-/-}$ mice (Fig. 2E–H). Periodic acid Schiff (PAS) staining indicated that kidney injury and glomerular sclerosis were more severe in TRIM31$^{-/-}$ than in TRIM31$^{+/+}$ AngII-treated mice (Fig. 2F, G). Severe foot process fusion, proliferation of mesangial cells and matrix were observed in TRIM31$^{-/-}$ AngII-treated mice as indicated by transmission electron microscopy (Fig. 2I). These data indicated that TRIM31 deficiency promoted AngII-induced kidney injury.

TRIM31 deficiency promoted AngII-induced hypertensive kidney fibrosis and inflammation in vivo

As fibrosis is a salient feature of hypertension-induced chronic kidney injury and other organs [6, 45], we quantified total collagen in TRIM31$^{+/+}$ and TRIM31$^{-/-}$ mice kidneys by picrosirius red and Masson's staining. Collagen expression in saline-treated mice were similar in TRIM31$^{+/+}$ and TRIM31$^{-/-}$ mice. After AngII infusion, the renal collagen content was significantly higher in TRIM31$^{-/-}$ than in TRIM31$^{+/+}$ mice. IHC for Collagen I and IV, fibronectin, and profibrotic α-smooth muscle actin (α-SMA) revealed severe fibrosis in kidneys of TRIM31$^{-/-}$ AngII-treated mice (Fig. 3A, B). Western blot and RT-PCR revealed similar changes in renal protein (Fig. 3C) and mRNA levels (Fig. 3F) of four mouse groups. These findings suggested that TRIM31 contributed to fibrosis in the hypertensive kidney in vivo.

Meso Scale Discovery (MSD) examination revealed that serum levels of TNF-α, IL-6 and IL-1β were similar between TRIM31$^{+/+}$ and TRIM31$^{-/-}$ saline-treated mice, and were markedly increased after AngII infusion. However, compared to the levels in TRIM31$^{+/+}$ AngII-treated mice, serum levels of IL-6, TNF-α, and IL-1β were significantly higher in TRIM31$^{-/-}$ AngII-treated mice (Fig. 3D), which were supported by Western blot (Fig. 3C), IHC (Fig. 3A, B), and RT-PCR (Fig. 3E) findings. IHC for CD68 indicated stronger macrophage infiltration in TRIM31$^{-/-}$ than in TRIM31$^{+/+}$ AngII-treated mice (Fig. 3A, B). Thus, TRIM31 deficiency promotes AngII-induced kidney inflammation in vivo.

TRIM31 overexpression alleviated AngII-induced hypertensive kidney injury, fibrosis and inflammation in vivo

To further verify the causal relation between TRIM31 and AngII-induced HRD, we treated C57BL/6J mice with adeno-associated virus (AAV) 9 carrying Flag-TRIM31 (AAV-*TRIM31*) and AAV-Flag (AAV-control) as negative control by means of tail vein injection. Western blot analysis of mouse kidney tissues confirmed that *TRIM31* expression was upregulated in AAV-TRIM31 group versus the AAV-control group (Fig. 4A). Then, mice in the AAV9-control and AAV-*TRIM31* groups received AngII infusion or saline for 6 weeks. Neither SBP nor DBP showed a significant difference between the two groups of mice after AngII treatment by radiotelemetry analysis (Fig. 4B). In contrast, serum levels of BUN, Cr and UA, 24-h urine albumin contents (Fig. 4C), glomerular sclerosis index and renal KIM-1 expression levels were all significantly decreased whereas nephrin expression was markedly increased in the AAV-TRIM31 group relative to the AAV9-control group (Fig. 4D–G). Transmission electron microscopy showed lessened fracture and fusion of foot process in the AAV-*TRIM31* mice relative to the AAV-control mice after AngII treatment (Fig. 4H). In addition, expression levels of Collagen I, Collagen III and Collagen IV, Fibronectin and α-SMA in renal tissues, which reflect the severity of renal fibrosis, were siginificaly reduced in the AAV-TRIM31 mice in comparison with the AAV-control mice after AngII treatment. Similarly, expression levels of TNF-α, IL-6, and IL-1β in renal tissues, which are parameters of renal inflammation, were remarkably attenuated in the AAV-TRIM31 mice versus the AAV-control mice after AngII treatment (Fig. 4I–K). Taken together, these results indicated that TRIM31 overexpression relieved AngII-induced kidney injury, fibrosis and inflammation in mice.

TRIM31 was involved in TGF-β1-mediated fibrosis and inflammation in vitro, and Smad, non-Smad signal pathway activation

TGF-β1 is a key profibrotic cytokine in hypertensive renal injury and tubulointerstitial fibrosis [6]. Western blot, IHC, and RT-PCR revealed that TGF-β1 expression in the kidneys obviously increased after AngII infusion, however, no statistical difference was observed between TRIM31$^{+/+}$ and TRIM31$^{-/-}$ mice

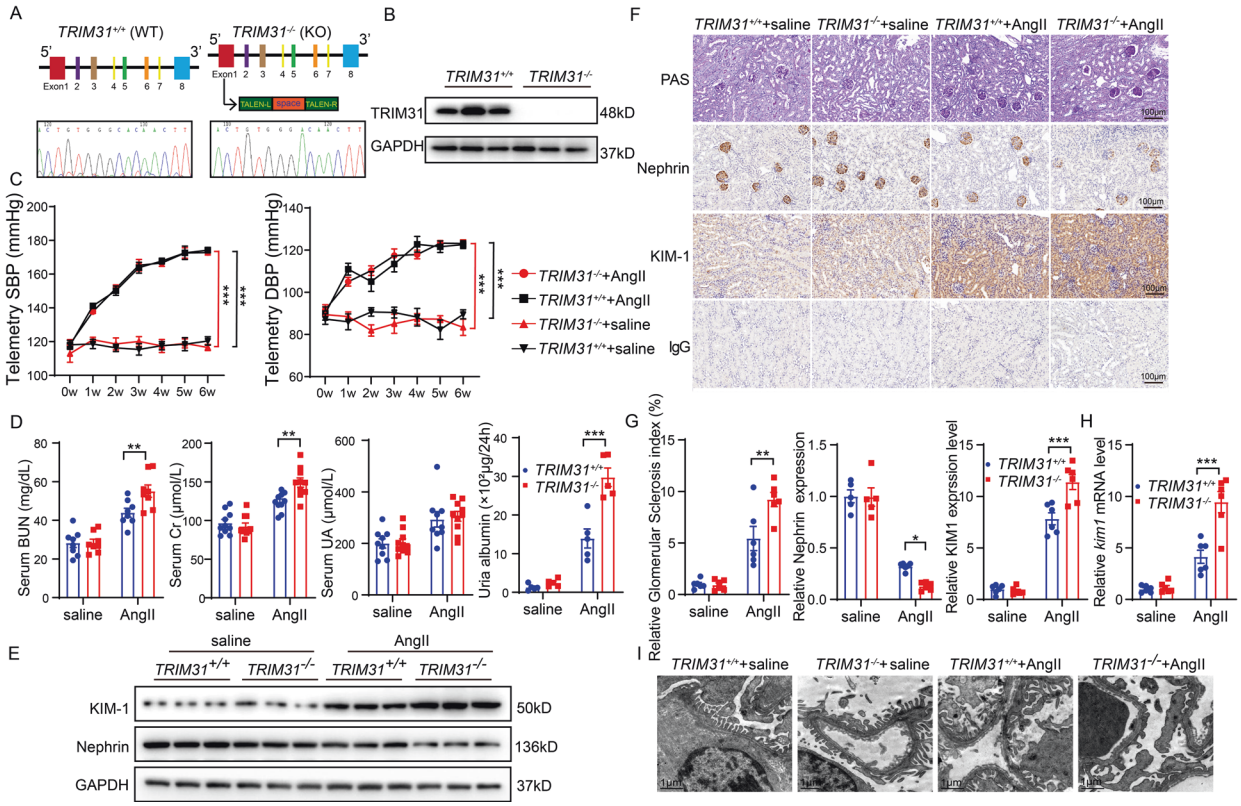

Fig. 2 TRIM31 deficiency aggravated AngII-induced kidney injury. A Generation of TRIM31$^{-/-}$ mice by targeting *TRIM31* exon1 using transcription activator-like effector nuclease technology and sequencing analysis of genomic DNA isolated from the tails of TRIM31$^{+/+}$ and TRIM31$^{-/-}$ mice. **B** Representative Western blot images of TRIM31 levels in TRIM31$^{+/+}$ and TRIM31$^{-/-}$ kidney tissues. **C** Changes in SBP and DBP measured by radiotelemetry of TRIM31$^{+/+}$ and TRIM31$^{-/-}$ mice treated with saline or AngII for 42 days. $n = 6$ per groups. **D** BUN ($n = 8$ per group), serum Cr ($n = 10$ per group), serum uric acid (UA) ($n \geq 9$ per groups), and 24-h urine albumin ($n = 5$ per group) levels in TRIM31$^{+/+}$ and TRIM31$^{-/-}$ mice treated with saline or AngII for 42 days. **E** Representative Western blot images of nephrin and KIM-1 in kidneys of the four mouse groups. **F**, **G** Representative PAS ($n = 6$ per group) and IHC staining of Nephrin ($n \geq 5$ per group) and KIM-1 ($n = 6$ per group) in kidneys of the four mouse groups, and quantitative analysis. **H** Relative *kim-1* mRNA levels in the four mouse groups, and quantitative analysis. $n = 6$ per group. **I** Representative photomicrographs showing typical glomerular structural changes in kidneys of the four mouse groups. Data were presented as mean ± SEM and normal distributions were tested by Shapiro–Wilk method, which showed that all data were normally distributed. Two-way ANOVA followed by Tukey post hoc test was used. Adjusted *P* values were provided in case of multiple groups comparisons. * adjusted $P < 0.05$, ** adjusted $P < 0.01$, *** adjusted $P < 0.001$. Each experiment was repeated independently for a minimum three times.

(Supplementary Fig. S2A–D). That means TRIM31 did not affect AngII-induced TGF-β1 production. Next, we investigated the effect of TGF-β1 on TRIM31 expression. In HK2 cells stimulated with hTGF-β1 for various times and at different concentrations, TRIM31 protein and mRNA levels were significantly decreased (Supplementary Fig. S2E–G). And TRIM31 degradation by AngII were prevented by blocking TGF-β1 with a neutralizing antibody (Supplementary Fig. S2H), which indicated that TRIM31 is directly induced by TGF-β1 and may be involved in TGF-β1-mediated tubulointerstitial fibrosis and hypertensive kidney injury in AngII pumping mice. Renal tubular epithelial cells are involved in the development of HRD by mediating inflammation and fibrosis, and the above data shown that the expression of TRIM31 decreased obviously in renal tubular epithelial cells under the stimulation of AngII or TGF-β1. To further explore the potential role of TRIM31 in TGF-β1 signaling, we knocked down TRIM31 in HK2 cells using small interfering (si)RNA. Endogenous TRIM31 mRNA and protein levels were significantly reduced in cells transfected with TRIM31-siRNA (si-TRIM31) compared to those in control (NC) siRNA-transfected cells. TRIM31 knockdown significantly decreased hTGF-β1-induced protein and mRNA expression of fibrotic factors, including collagens I, III, IV, fibronectin, α-SMA, matrix metalloproteinase (MMP) 2, and MMP9, and inflammatory factors, including TNF-α, IL-6, and IL-1β (Fig. 5A–C).

Next, we transfected HK2 cells with plasmids for TRIM31 overexpression, a deletion mutant TRIM31-ΔRing (lacking the Ring domain, which confers E3 ubiquitin ligase activity), or mutants in which the conserved cysteine residues at positions 53 and 56 within the Ring domain were replaced with alanine (TRIM31-C53A/C56A). TRIM31 overexpression suppressed hTGF-β1-induced protein and mRNA expressions of fibrotic and inflammatory factors. These effects of TRIM31 overexpression were abolished after transfection of TRIM31-ΔRing or TRIM31-C53A/56A (Fig. 5D–E, Supplementary Fig. S3). These data suggested an essential role of Ring domain and E3 ligase activity of TRIM31 in counteracting the profibrotic and proinflammatory effects of hTGF-β1.

Activation of canonical and non-canonical Smad signaling pathways, especially the NF-κB and MAPK pathways, is crucial in the pathogenesis of tubulointerstitial fibrosis. After AngII infusion, Smad2 and Smad3 activations in the kidneys were significantly upregulated, especially in TRIM31$^{-/-}$ AngII-treated mice. Phosphorylation of P65, ERK, JNK, and P38 in the AngII-treated mice kidneys were also increased in TRIM31$^{-/-}$ compared to TRIM31$^{+/+}$ (Fig. 5F). pSmad2, pSmad3, pP65, pERK, pJNK, and pP38 levels were increased in HK2 cells treated with hTGF-β1 for 0.5 h or 1 h (Fig. 5G). These data indicated that TRIM31 regulated TGF-β1-mediated Smad and non-Smad signaling activation.

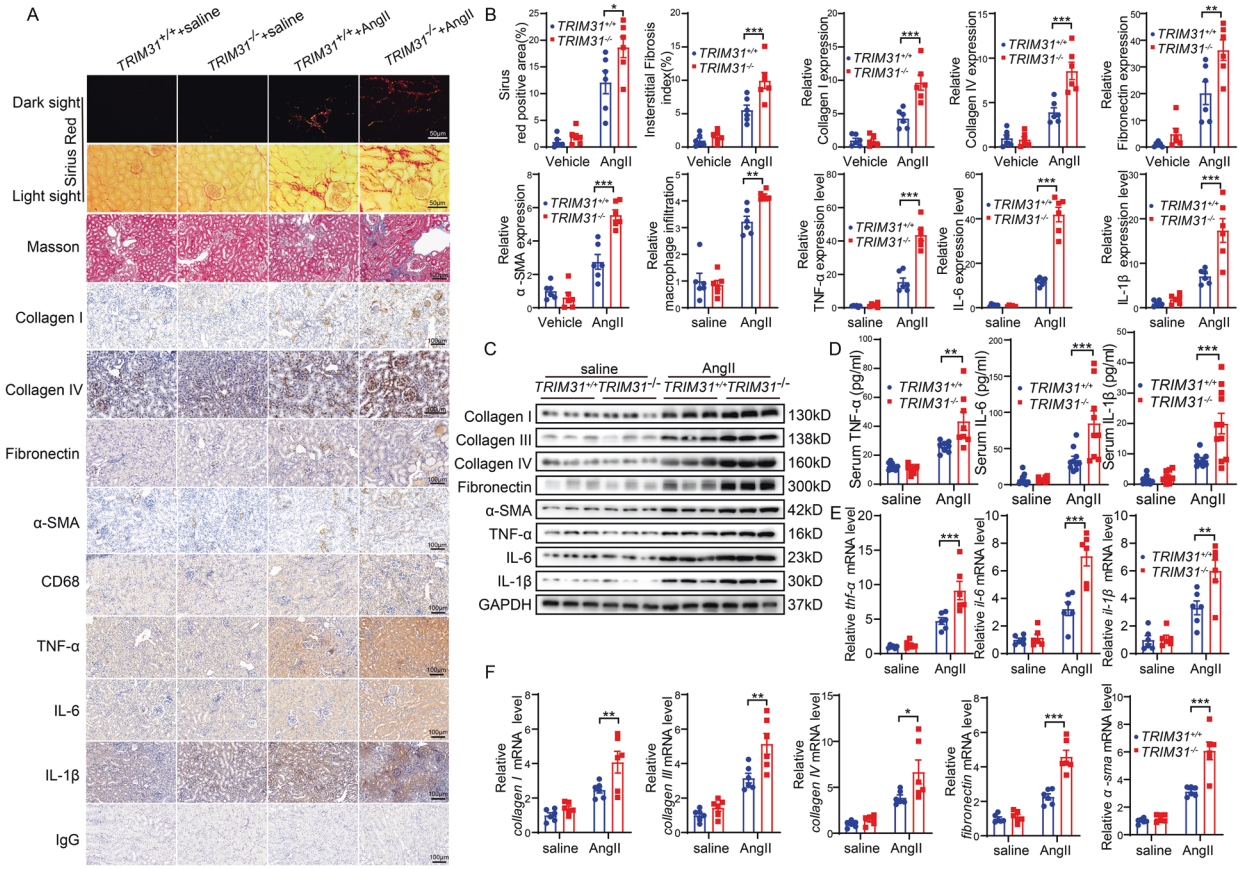

Fig. 3 TRIM31 deficiency promoted AngII-induced hypertensive kidney fibrosis and inflammation in vivo. A, B Representative images of Sirius red, Masson and IHC staining of Collagen I and IV, Fibronectin, α-SMA, TNF-α, IL-6, and IL-1β and quantitation in TRIM31$^{+/+}$ and TRIM31$^{-/-}$ mouse kidneys treated with saline or AngII for 42 days. $n = 6$ per group. **C** Representative Western blot images of Collagen I, III and IV, Fibronectin, α-SMA, TNF-α, IL-6, and IL-1β in kidneys of the four mouse groups. GAPDH was used for normalization. **D** MSD assay showing serum levels of TNF-α ($n = 8$ per group), IL-6 ($n = 10$ per group), IL-1β ($n = 10$ per group), and MCP1 ($n = 10$ per group) in TRIM31$^{+/+}$ and TRIM31$^{-/-}$ mice treated with saline or AngII for 42 days. **E** Relative mRNA levels of *tnf-α*, *il-6*, and *il-1β* in kidneys of the four mouse groups. $n = 6$ per group. **F** Relative mRNA levels of *collagen I*, *III* and *IV*, *fibronectin*, and *α-sma* in kidneys of the four mouse groups. $n = 6$ per group. Data were presented as mean ± SEM and normal distributions were tested by Shapiro–Wilk method, which showed that all the data were normally distributed. Two-way ANOVA followed by Tukey post hoc test was used. Adjusted *P* values were provided in case of multiple groups comparisons. * adjusted $P < 0.05$, ** adjusted $P < 0.01$, *** adjusted $P < 0.001$. Each experiment was repeated independently for a minimum three times.

TRIM31 targeted MAP3K7 for its proteasomal degradation

To identify molecules regulated by TRIM31, we transfected HEK293T cells with various downstream targets overexpression plasmids of TGF-β1 signaling and used the cells for co-immunoprecipitation (Co-IP) experiments. TRIM31 was associated with TRAF6 and MAP3K7, but not with Smad2, Smad3, and Smad4 (Fig. 6A, B, Supplementary Fig. S4A). Endogenous Co-IP experiments in HK2 cells confirmed the interactions between endogenous TRIM31 and TRAF6 and MAP3K7, and the interaction between TRIM31 and MAP3K7 increased over time after hTGF-β1 stimulation (Fig. 6C). To evaluate the effect of TRIM31 on the functions of these targets, we transfected HEK293T cells with Myc-MAP3K7 or Myc-TRAF6 and a concentration gradient of Flag-TRIM31 plasmid. TRIM31 markedly degraded MAP3K7 (Fig. 6D), which was abolished by TRIM31-ΔRing and TRIM31-C53A/56 A transfection (Fig. 6E), but it did not significantly affect TRAF6 levels (Supplementary Fig. S4B). Thus, we considered MAP3K7 as a target of TGF-β1 downstream signal molecule for TRIM31.

As ubiquitin-proteasome system and autophagy-lysosome pathway are the two most important mechanisms for the repair or removal of abnormal proteins [32], we investigated which of these two pathways is involved in TRIM31-induced MAP3K7 degradation by treating HEK293T cells with the proteasome inhibitor bortezomib or the lysosomal pathway inhibitor chloroquine. MAP3K7 degradation was obviously abolished after bortezomib treatment, indicating that TRIM31-induced MAP3K7 degradation via the proteasome pathway (Fig. 6F). Confocal microscopy revealed that TRIM31 colocalized with MAP3K7 in HEK293T cells (Fig. 6G). To verify that TRIM31 associates with MAP3K7, we produced Flag-tagged MAP3K7 and Myc-tagged TRIM31 recombinant proteins using an in vitro TNT protein expression system for Co-IP assays. Myc-TRIM31 co-immunoprecipitated with Flag–MAP3K7, indicating that TRIM31 interacted with MAP3K7 in vitro (Fig. 6H). A glutathione S-transferase (GST) pull-down assay indicated that TRIM31 binded to MAP3K7 via a direct interaction (Supplementary Fig. S4C).

To explore the binding domains required for TRIM31–MAP3K7 interaction, we constructed several TRIM31 deletion mutants of the Ring-finger domain (amino acids (aa) 16–57), B-box (aa 90–129), or C-C motif (aa 126–307) (Fig. 6I), and used them in Co-IP experiments. TRIM31-ΔC-C and TRIM31-ΔC had lost the ability to interact with MAP3K7. Points mutants of TRIM31 (C53A/C56A) also interacted with MAP3K7 (Fig. 6J). Using a series of MAP3K7 deletion mutants (Fig. 6K) we found that the amino-terminal 300 aa of MAP3K7 are required for TRIM31–MAP3K7 binding (Fig. 6L).

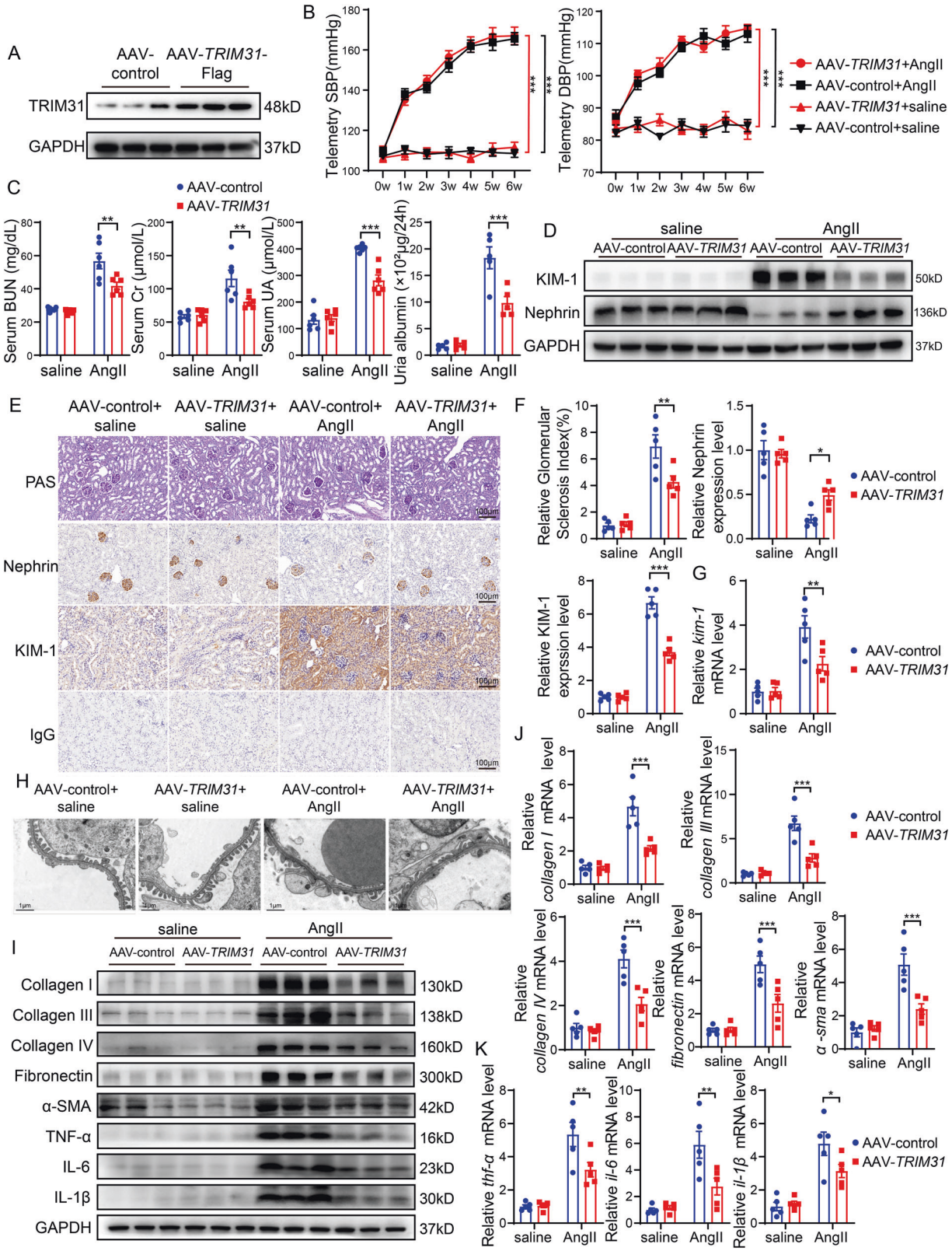

These data demonstrated that TRIM31 physically interacted with MAP3K7 and that aa 130–425 of TRIM31 and aa 1–300 of MAP3K7 were involved in the binding process. Thus, TRIM31 directly interacted with MAP3K7 and mediated proteasomal degradation of MAP3K7.

TRIM31 catalyzed K48-linked polyubiquitination of MAP3K7

For the proteins proteasomal degradation was always associated with ubiquitination modification, we next investigated whether TRIM31 regulates the ubiquitination of MAP3K7 through its E3 ligase activity. We transfected HEK293T cells with Myc-tagged

Fig. 4 TRIM31 overexpression alleviated AngII-induced hypertensive kidney injury, fibrosis and inflammation in vivo. A Representative Western blot images of TRIM31 expression in AAV-control and AAV-*TRIM31*-Flag kidney tissues. **B** Temporal changes in SBP and DBP measured by radiotelemetry in AAV-control and AAV-*TRIM31* mice treated with saline or AngII for 42 days. $n = 5$ per groups. **C** Serum BUN ($n = 6$ per group), Cr ($n = 6$ per group), UA ($n = 6$ per groups), and 24-h urine albuminuria ($n = 5$ per group) levels in AAV-control and AAV-*TRIM31* mice treated with saline or AngII for 42 days. **D** Representative western blot images of nephrin and KIM-1 expression in kidneys of the four mouse groups. **E**, **F** Representative PAS staining ($n = 5$ per group) and IHC staining of nephrin ($n = 5$ per group) and KIM-1 ($n = 5$ per group) in kidneys of the four mouse groups, and corresponding quantitative analyses. **G** Relative *kim-1* mRNA levels in the four mouse groups. $n = 5$ per group. **H** Representative photomicrographs showing typical glomerular structural changes in kidneys of the four mouse groups. **I** Representative Western blot images of Collagen I, III and IV, fibronectin, α-SMA, TNF-α, IL-6, and IL-1β in kidneys of the four mouse groups. GAPDH was used for normalization. **J**, **K** Relative mRNA levels of *collagen I*, *III* and *IV*, *fibronectin*, *α-sma*, *tnf-α*, *il-6*, and *il-1β* in kidneys of the four mouse groups. $n = 5$ per group. Data were presented as mean ± SEM and normal distributions were tested by Shapiro–Wilk method, which showed that all data were normally distributed. Two-way ANOVA followed by Tukey post hoc test was used. Adjusted *P* values were provided in case of multiple groups comparisons. * adjusted $P < 0.05$, ** adjusted $P < 0.01$, *** adjusted $P < 0.001$. Each experiment was repeated independently for a minimum three times.

MAP3K7, HA-tagged ubiquitin, and Flag-tagged TRIM31 expression plasmids. MAP3K7, but not TRAF6, was significantly polyubiquitinated by TRIM31 (Supplementary Fig. S5). TRIM31-(C53A/C56A) and TRIM31-ΔRing lost the ability to increase MAP3K7 polyubiquitination (Fig. 7A), indicating that MAP3K7 can be ubiquitinated by TRIM31 via its E3 ligase activity. To investigate the type of polyubiquitination mediated by TRIM31, we transfected cells with plasmids expressing HA-tagged mutant ubiquitin (K48 or K63), in which all lysine residues except K48 or K63, are substituted with arginine. Polyubiquitination of MAP3K7 was catalyzed by TRIM31 in the presence of HA-tagged WT ubiquitin and HA-ubiquitin (K48), but not HA-ubiquitin (K63) (Fig. 7B). Next, we measured TRIM31-induced ubiquitination of endogenous MAP3K7 in cells transfected with NC or si-TRIM31 after hTGF-β1 stimulation. Endogenous MAP3K7 was robustly ubiquitinated, with both K48- and K63-linked chains. The total amount of WT and K48-linked ubiquitination of MAP3K7 was much lower in si-TRIM31 than in NC cells, whereas K63-linked ubiquitination of MAP3K7 was not substantially different (Fig. 7C).

Next, we identified the lysine residues responsible for TRIM31-mediated polyubiquitination of MAP3K7. MAP3K7-K72 [41, 42] and MAP3K7-K158 [39, 46] are reportedly associated with K48- or K63-linked ubiquitination of MAP3K7, respectively, but the E3 ligase was not identified. Therefore, we verified whether MAP3K7-K72 and K158 are involved in the ubiquitination of MAP3K7 by TRIM31. K48-linked ubiquitination of MAP3K7 by TRIM31 was obviously abolished after MAP3K7-K72R transfection (Fig. 7D). Then, we generated the mutant MAP3K7-KR, in which all lysine residues were replaced with arginine, and reintroduced lysine residues into MAP3K7-KR to generate single-lysine mutant MAP3K7-K72. Cotransfection and Co-IP analyses of HEK293T cells showed that TRIM31-induced K48-linked polyubiquitination of MAP3K7-WT and the MAP3K7-K72 mutant (Fig. 7E). However, MAP3K7-K72 did not undergo K63-linked polyubiquitination in the presence of TRIM31 (Fig. 7F).

In vitro ubiquitination assays using ubiquitin, ubiquitin-activating enzyme E1, and ubiquitin-conjugating enzyme UbcH5a were performed to confirm that TRIM31 promotes K48-linked polyubiquitination of MAP3K7. TRIM31 catalyzed MAP3K7 polyubiquitination in the presence of ubiquitin (WT). Next, we conducted in vitro ubiquitination assays using mutant ubiquitin(K48) or (K63), which contains only one lysine, K48 or K63, with all other lysines mutated to arginine. MAP3K7 was ubiquitinated by TRIM31 in the presence of ubiquitin (WT) and ubiquitin(K48), but not in the presence of ubiquitin(K63) (Fig. 7G). When we expressed Myc-tagged MAP3K7-K72 and Myc- MAP3K7-K72R in an in vitro TNT protein expression system, we found that TRIM31 polyubiquitinated MAP3K7-WT and MAP3K7-K72, but not MAP3K7-K72R (Fig. 7H). These findings confirmed the key role of TRIM31 in K48-linked ubiquitination of K72 residue on MAP3K7.

TRIM31- MAP3K7-Smad/non-Smad pathways played important roles in HRD

Next, we investigated the function of MAP3K7 in the progression of HRD. Upon treatment of HK2 cells with the MAP3K7 inhibitor 5z-7-oxozeaenol (5z7) [47, 48], hTGF-β1-mediated phosphorylation of canonical Smad and non-Smad pathway molecules, including NF-κB and MAPK (ERK, JNK, P38), was significantly abolished (Fig. 8A). In addition, siRNA-mediated MAP3K7 knockdown significantly decreased hTGF-β1-induced phosphorylation of NF-κB, ERK, JNK, and P38 (Fig. 8B). Similar observations were made in mouse primary renal tubular epithelial cells (MRPTEpiC) (Supplementary Fig. S6A, B). These results suggested that inhibition of MAP3K7 activity in renal tubular epithelial cells affected the activation of both Smad and non-Smad signaling pathways.

IHC of Control, GML, and HRD kidney sections revealed significant upregulation of TGF-β1 in HRD patients. Fibrosis-related Collagen I and inflammation-related TNF-α were also detected in HRD sections. The levels of pSmad3 and pP65, which are classic pro-fibrotic and pro-inflammatory signaling proteins stimulated by TGF-β1, were also increased in HRD sections. MAP3K7 as a target of TRIM31, was significantly upregulated in HRD sections (Fig. 8C, D). These results suggested that TRIM31 may play an important role in HRD via regulating MAP3K7.

DISCUSSION

As an important E3 ubiquitin ligase, TRIM31 plays key roles in broad range of biological events, especially, in the innate immune response [31], NLRP3 inflammasome activation [32], intestinal microbiota composition [33], and intestinal autophagy [34, 35]. However, whether it plays a role in HRD and its underlying mechanism remain unclear. The present study revealed a previously unrecognized biological function of TRIM31 in the suppression of HRD in human and mice. We generated TRIM31$^{-/-}$ mice and chronically administered AngII, which is involved in the regulation of blood pressure and electrolyte balance, to establish a mouse model of HRD [4, 33]. We found that TRIM31 were significantly down-regulated in AngII -treated mouse renal tissues, especially in renal tubules. We collected tissues from patients with HRD and found that TRIM31 was significantly down-regulated with the progression of HRD. These results suggest that TRIM31 may play an important role in the progression of HRD.

Glomerular proteinuria is a typical laboratory finding of chronic kidney disease, and podocytes play a prominent role in maintaining glomerular filter integrity [15, 49]. Herein, renal functional impairment, fibrosis, and inflammation in mice with AngII-induced HRD were substantially aggravated by TRIM31 ablation and alleviated by TRIM31 overexpression. Furthermore, compared with TRIM31$^{+/+}$ AngII-treated mice, the elevation of 24-h urine albumin contents was more pronounced, and the glomerular and tubular damage was more severe in TRIM31$^{-/-}$

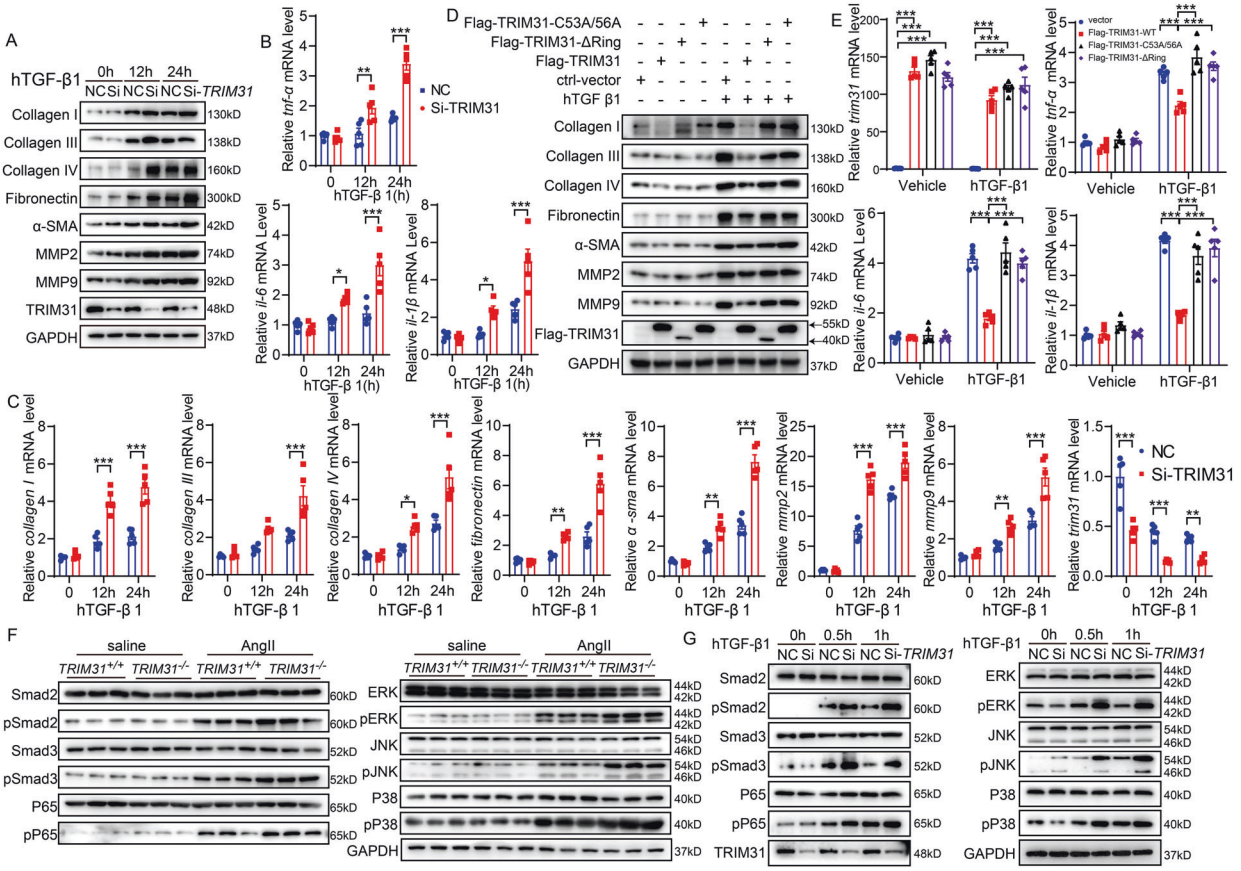

Fig. 5 TRIM31 was involved in TGF-β1-mediated fibrosis and inflammation in vitro and in Smad and non-Smad signal pathway activation. **A** Representative Collagen I, III and IV, Fibronectin, α-SMA, MMP2, MMP9, TNF-α, IL-6, and IL-1β western blot images in HK2 cells stimulated with TGF-β1 (10 ng/mL) for 12 h or 24 h, after normal control (NC) and si-TRIM31 transfections. **B** Relative *tnf-α*, *il-6*, and *il-1β* mRNA levels in HK2 cells in the aforementioned six groups. $n = 5$ per group. **C** Relative *collagen I*, *III* and *IV*, *fibronectin*, *mmp2*, *mmp9*, *α-sma*, and *trim31* mRNA levels in HK2 cells in aforementioned six groups. $n = 5$ per group. **D** Representative collagen I, III and IV, fibronectin, α-SMA, MMP2, MMP9, and Flag Western blot images in HK2 cells stimulated with TGF-β1 for 24 h and transfected with control vector, TRIM31, TRIM31-C53A/56A, or TRIM31-ΔRing expression plasmid. **E** Relative *tnf-α*, *il-6*, *il-1β*, and *trim31* mRNA levels in HK2 cells of eight groups. $n = 5$ per group. **F** Representative Western blot images of Smad2, Smad3, P65, ERK, JNK, and P38 phosphorylation levels in TRIM31$^{+/+}$ and TRIM31$^{-/-}$ mouse kidneys treated with saline or AngII for 42 days. **G** Representative Western blot images of Smad2, Smad3, P65, ERK, JNK, and P38 phosphorylation levels in HK2 cells stimulated with TGF-β1 (10 ng/mL) for 0.5 h or 1 h after NC and si-TRIM31 transfections. GAPDH was used for normalization. Data were presented as mean ± SEM and normal distributions were tested by Shapiro–Wilk method, which showed that all the data were normally distributed. Two-way ANOVA followed by Sidak post hoc test was used for **B** and **C**. Two-way ANOVA followed by Tukey post hoc test was used for **E**. Adjusted *P* values were provided in case of multiple groups comparisons. * adjusted $P < 0.05$, ** adjusted $P < 0.01$, *** adjusted $P < 0.001$. Each experiment was repeated independently for a minimum three times.

AngII-treated mice. On the contrary, the opposite phenotype changes were found in AAV-*TRIM31* AngII-treated mice, suggesting that TRIM31 may play an important role in alleviating podocyte dysfunction and tubular damage in HRD. However, SBP and DBP were not affected by TRIM31 deletion or overexpression, indicating that TRIM31 protects mice from HRD via direct targeting effects rather than altering their blood pressure. These results further prove that TRIM31 plays an important protective role in AngII-induced HRD, which inspired us to further investigate the targets and molecular mechanisms of TRIM31.

To study the TRIM31 function during HRD development, we focused on TGF-β1 as it plays essential roles in various kidney diseases, including AngII-induced HRD [6, 18]. We observed a significant increase of TGF-β1 in human and mouse hypertensive kidneys, however, TGF-β1 expression was not affected by TRIM31 knockout. Meanwhile, in HK2 cells [2], TGF-β1 stimulation significantly decreased TRIM31 expression, which was consistent with the change in TRIM31 expression in the disease model. Further, the E3 ligase activity of TRIM31 is essential for antagonizing hTGF-β1-induced fibrosis and inflammation. To explore the mechanism of these beneficial effects, we focused on downstream factors of TGF-β1 signaling. Interestingly, TRIM31 deficiency dramatically promoted the phosphorylation and activation of canonical Smad-dependent and non-canonical Smad-independent (NF-κB/MAPK) signaling pathways in vivo and in vitro.

To discover targets of TRIM31, we overexpressed various TGF-β1 downstream molecules. Co-IP assays revealed that TRIM31 binded to TRAF6 and MAP3K7 but not to Smad2/3/4. Further proteasomal degradation, GST pull-down assay and confocal microscopy experiments revealed that MAP3K7 is a target of TRIM31 in the TGF-β1 signaling pathway. We also found the binding domains responsible for the TRIM31-MAP3K7 interaction.

Protein ubiquitination is essential for proteasomal degradation, and MAP3K7 could be ubiquitinated through both K48 and K63 linkages. The identification of TRIM31 as a MAP3K7-associated protein prompted us to investigate whether TRIM31-mediated MAP3K7 ubiquitination. Ubiquitin is composed of 76 amino acids, and each lysine residue can be coupled to the c-terminal Gly residue of ubiquitin to form a polyubiquitin chain [30, 50]. As K48-linked polyubiquitination usually leads to target degradation via the 26S proteasome, and K63-linked polyubiquitination is involved

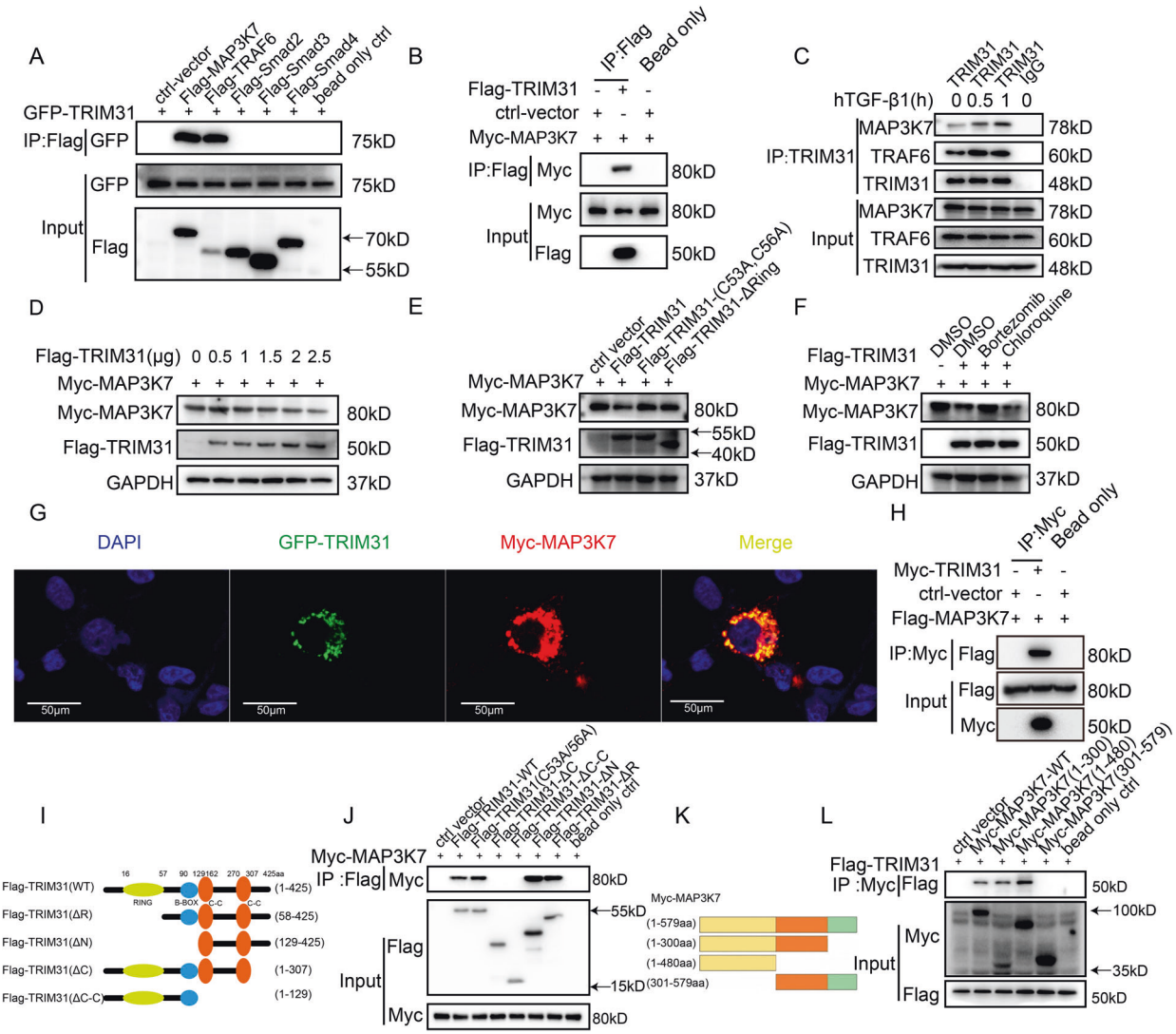

Fig. 6 TRIM31 targeted MAP3K7 for its proteasomal degradation. A Co-IP assay of HEK293T cells cotransfected with GFP-TRIM31 and Flag-tagged-MAP3K7, TRAF6, Smad2, Smad3, and Smad4 to examine interactors of TRIM31. **B** Co-IP assay of HEK293T cells cotransfected with Flag-TRIM31 and Myc-MAP3K7 to examine whether TRIM31 interacts with MAP3K7. **C** Co-IP assay of HK2 cells to examine whether endogenous TRIM31 interacts with MAP3K7 and TRAF6. **D** Representative Western blot images of Myc-MAP3K7 in HEK293T cells transfected with a concentration gradient of Flag-TRIM31. **E** Western blot of Myc-MAP3K7 protein in HEK293T cells transfected with Flag-TRIM31(WT) and mutants. **F** Representative Western blot images of Myc-MAP3K7 in HEK293T cells transfected with Flag-TRIM31 and pretreated with bortezomib (100 nmol/L) and chloroquine (5 μmol/L) for 4 h. **G** Representative confocal microscopic images of colocalization of TRIM31 and MAP3K7 in HEK293T cells. **H** In vitro Co-IP analysis of TRIM31–MAP3K7 interaction, using Flag-MAP3K7 and Myc-TRIM31. **I**, **J** Schematic representations of human TRIM31(WT) and its truncation mutants, and Co-IP analysis of the interaction of Myc-MAP3K7 with Flag-TRIM31 (WT), the TRIM31 truncation mutants, and Flag-TRIM31(C53A, C56A) in HEK293T cells. **K**, **L** MAP3K7(WT) and its truncation mutants, and Co-IP analysis of the interaction between Flag–TRIM31 and Myc-MAP3K7 or its truncation mutants in HEK293T cells. Each experiment was repeated independently for a minimum three times.

in signal transduction and trafficking of targeted proteins, these two are the most common types of ubiquitination [51]. Endogenous and exogenous ubiquitination, as well as in vitro ubiquitination assays revealed that MAP3K7 was ubiquitinated by TRIM31 through its E3 ligase activity in the way of K48-linked ubiquitination, which reportedly promotes protein degradation via the 26S proteasome pathway. These results were in line with previous reports on MAP3K7 degradation by TRIM31. K72 and K158 of MAP3K7 are closely associated with its ubiquitination, and are responsible for K48- and K63-linked polyubiquitination, respectively [39, 41, 46, 52]. We, therefore, constructed K72R, K158R, KR, and K72 mutants to verify which residues are involved in MAP3K7 ubiquitination by TRIM31. Interestingly, TRIM31 catalyzed the K48-linked polyubiquitination of MAP3K7-WT, MAP3K7-K158R, and MAP3K7-K72, but not that of MAP3K7-K72R, and MAP3K7-K72 did not mediate K63-linked polyubiquitination in the presence of TRIM31. Together, these findings confirmed a key role of TRIM31 in the ubiquitination of MAP3K7 at K72 for the first time.

We further investigated the function of MAP3K7 in HRD as it has been reported previously that MAP3K7 regulates the activation of TGF-β-mediated non-Smad signaling, especially NF-κB/MAPKs [29, 47]. However, the role of MAP3K7 in TGF-β1-mediated Smad-dependent signaling is controversial. Some studies have shown that it is not involved in regulating the activation of Smad signaling [23], while others believe that it is. Using HK2 and mouse primary renal tubular epithelial cells treated with the MAP3K7 inhibitor 5z7 [25, 37] and siRNA-

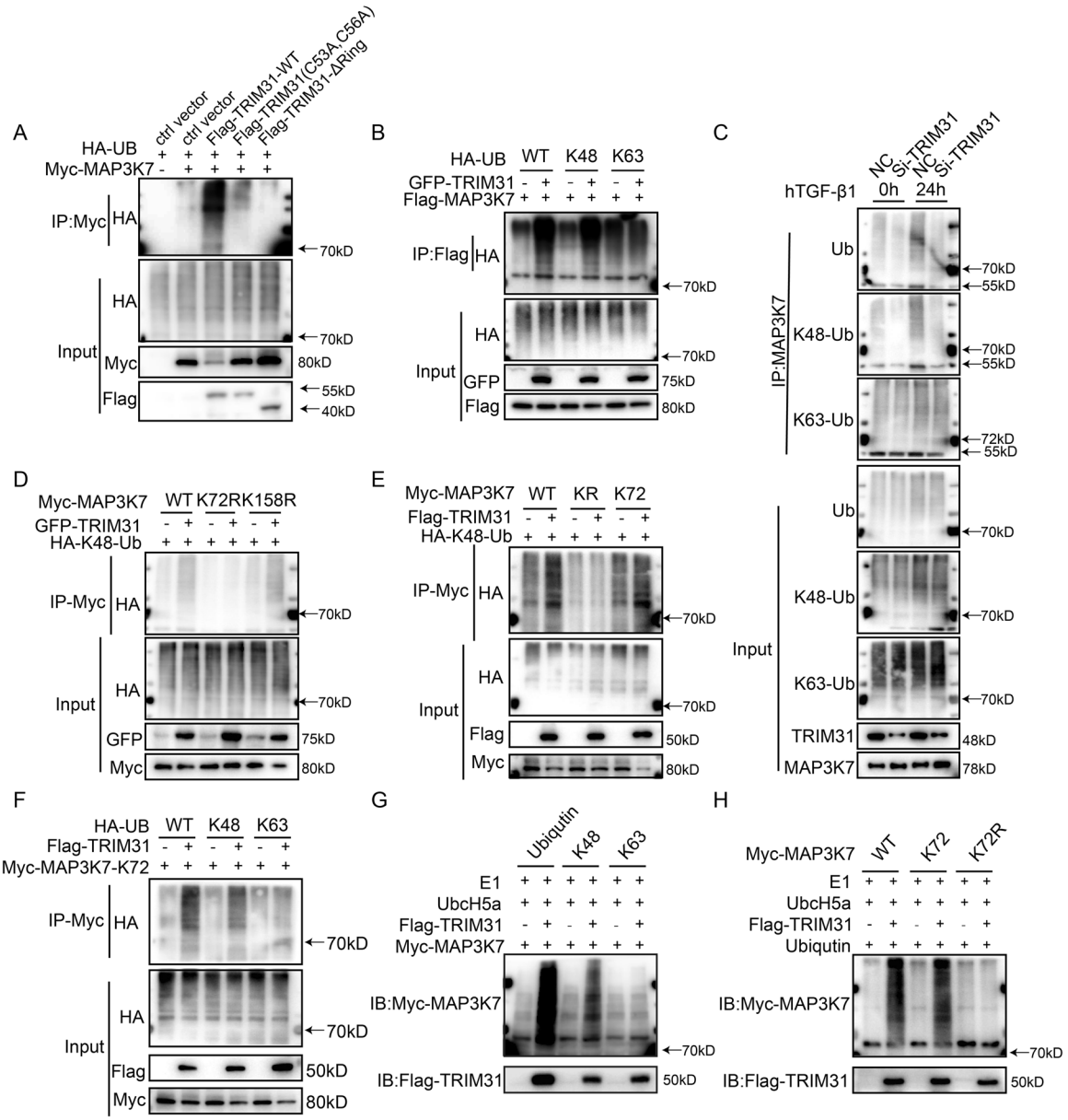

Fig. 7 TRIM31 catalyzed K48-linked polyubiquitination of MAP3K7. A Co-IP analysis of MAP3K7 ubiquitination in HEK293T cells transfected with plasmids encoding Myc-MAP3K7 and HA-ubiquitin (WT), as well as a control vector or plasmids encoding Flag-TRIM31(WT), Flag-TRIM31-(C53A/C56A), or Flag-TRIM31-ΔRing. **B** Co-IP analysis of MAP3K7 ubiquitination in HEK293T cells transfected with plasmids expressing Myc-MAP3K7, GFP-TRIM31(WT), HA-ubiquitin (WT), HA-ubiquitin(K48), or HA-ubiquitin(K63). **C** Co-IP analysis of endogenous MAP3K7 ubiquitination in HK2 cells transfected with control siRNA (NC) or TRIM31-specific siRNA (si-TRIM31) after TGF-β1 (10 ng/mL) stimulation for 24 h. **D**, **E** Co-IP analysis of the polyubiquitination of MAP3K7(WT) and its mutants in HEK293T cells transfected with plasmids encoding Myc-tagged MAP3K7 (WT or mutant), plus GFP-TRIM31 and HA-ubiquitin(K48). **F** Co-IP analysis of mutant MAP3K7 ubiquitination in HEK293T cells transfected with plasmids expressing Myc-MAP3K7-K72, Flag-TRIM31(WT), and HA-ubiquitin (WT), HA-ubiquitin(K48), or HA-ubiquitin(K63). **G** In vitro MAP3K7-Ubiquitination assay with in vitro-translated Flag-TRIM31 and Myc-MAP3K7 in the presence of E1, UbcH5a, ubiquitin (WT), ubiquitin(K63) or ubiquitin(K48). **H** In vitro MAP3K7 ubiquitination assay with in vitro-translated Flag-TRIM31 and Myc-MAP3K7(WT), Myc-MAP3K7(K72), or Myc-MAP3K7(K72R), in the presence of E1, UbcH5a, and ubiquitin (WT). Each experiment was repeated independently for a minimum three times.

mediated MAP3K7 knockdown, we found that hTGF-β1-mediated phosphorylation of both the canonical Smad and non-Smad pathways were abolished. Further, MAP3K7 was significantly upregulated in human HRD kidney tissues, along with TGF-β1, collagen I, TNF-α, pSmad3, and pP65. These findings suggest the critical role of MAP3K7 in HRD progression in humans and mice.

Based on in vitro and in vivo HRD models, we found that TRIM31 acts as a negative regulator of functional and structural kidney fibrosis and inflammation by suppressing MAP3K7-pSmad2/3 and MAP3K7-NF-κB/MAPK signalings. Importantly, decreased TRIM31 expression and MAP3K7-Smad2/3/NF-κB/MAPK cascade activation were confirmed in human hypertensive kidneys. Mechanistically, in response to TGF-β1 stimulation, the direct binding of TRIM31 to MAP3K7 is enhanced, leading to MAP3K7 K48-linked polyubiquitination at K72 and subsequently, proteasomal degradation. MAP3K7 ubiquitination then leads to decreased phosphorylation and activation of the downstream

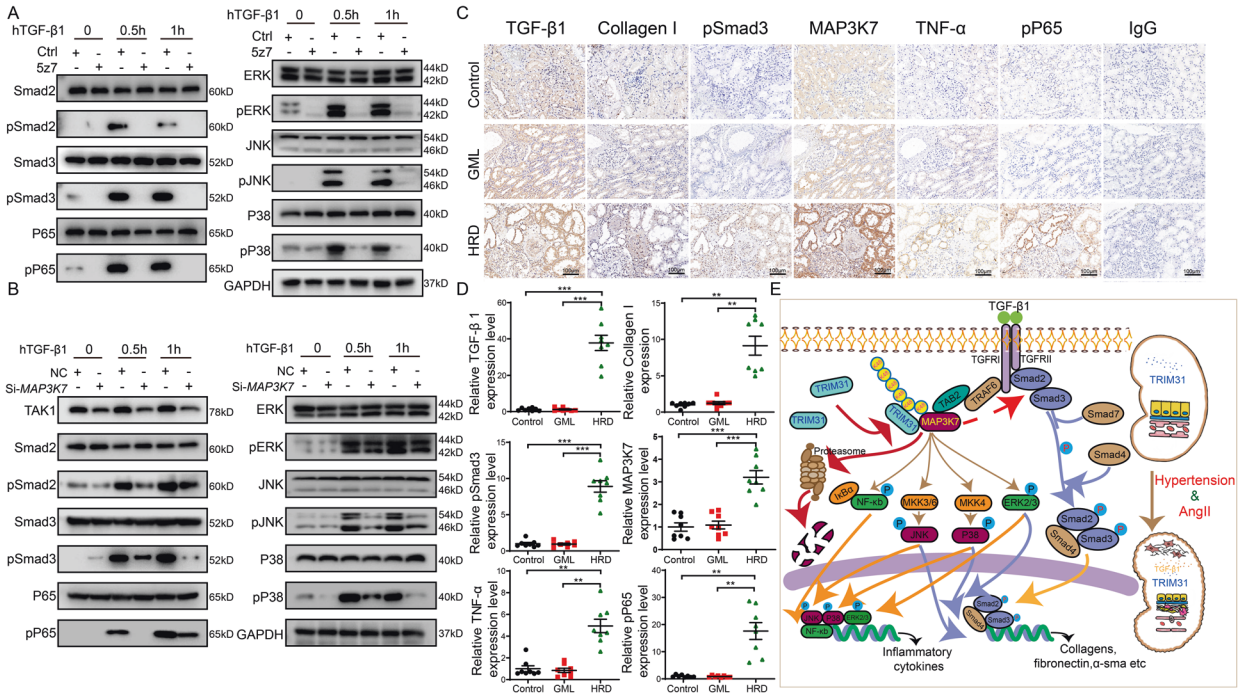

Fig. 8 TRIM31-MAP3K7-Smad/non-Smad pathways were involved in human and mouse HRD. A Representative Western blot images of Smad2, Smad3, P65, ERK, JNK, and P38 phosphorylation levels in HK2 cells pretreated with 5z7 (10 μmol/L) and stimulated with TGF-β1 (10 ng/mL) for 05.h or 1 h. **B** Representative Western blot images of Smad2, Smad3, P65, ERK, JNK, and P38 phosphorylation levels in HK2 cells pretreated with Si-NC and Si-MAP3K7 and stimulated with TGF-β1 (10 ng/mL) for 05.h or 1 h. **C**, **D** Representative photomicrographs and quantitation of IHC of TGF-β1, collagen I, pSmad3, MAP3K7, TNF-α, and pP65 in human renal cortical tissues obtained from the poles of healthy kidneys of individuals without kidney disease who underwent tumor nephrectomies (Control), patients with GML, and patients with HRD ($n = 8$ per group). **E** Under the condition of HRD, a reduction in TRIM31 leads to a decreased ubiquitylation of MAP3K7, thereby activating the TGF-β1-MAP3K7-pSmad2/3 and TGF-β1-MAP3K7-NF-κB/MAPK pathways, which contributes to kidney injury associated with hypertension. Data were presented as mean ± SEM and normal distributions were tested by Shapiro–Wilk method, which showed that MAP3K7 and pP65 were normally distributed, TGF-β1, collagen I, pSmad3 and TNF-α were not in **D**. One-way ANOVA followed by Dunnett post hoc test was used for **D** (MAP3K7 and pP65). Kruskal–Wallis test with Dunnett post hoc tests was used for **D** (TGF-β1, collagen I, pSmad3 and TNF-α). Adjusted P values were provided in case of multiple groups comparisons. * adjusted $P < 0.05$, ** adjusted $P < 0.01$, *** adjusted $P < 0.001$. Each experiment was repeated independently for a minimum three time.

Smad2/3 and NF-κB/MAPK signaling cascades (Fig. 8). This study demonstrated the functional role of TRIM31 in the process of HRD and the underlying mechanism.

In summary, we found here, the E3 ligase TRIM31 can promote the K48-linked ubiquitination at K72 and proteasomal degradation of MAP3K7, thereby negatively regulating the TGF-β1-mediated inflammatory response and renal fibrosis, and ultimately inhibiting the progression of HRD.

DATA AVAILABILITY

The datasets used and/or analyzed during the current study are available from the corresponding author on reasonable request

REFERENCES

1. Pan X, Shao Y, Wu F, Wang Y, Xiong R, Zheng J, et al. GF21 Prevents angiotensin II-induced hypertension and vascular dysfunction by activation of ACE2/Angiotensin-(1-7) axis in mice. Cell Metab. 2018;27:1323–37.
2. Meguid ENA, Bello AK. Chronic kidney disease: the global challenge. Lancet 2005;365:331–40.
3. Rucker AJ, Rudemiller NP, Crowley SD. Salt, hypertension, and immunity. Annu Rev Physiol. 2018;80:283–307.
4. Rodriguez-Iturbe B, Pons H, Johnson RJ. Role of the immune system in hypertension. Physiol Rev. 2017;97:1127–64.
5. Cravedi P, Ruggenenti P, Remuzzi G. Proteinuria should be used as a surrogate in CKD. Nat Rev Nephrol. 2012;8:301–6.
6. Meng X, Nikolic-Paterson DJ, Lan HY. TGF-β: the master regulator of fibrosis. Nat Rev Nephrol. 2016;12:325–38.
7. Xue Y, Lim S, Yang Y, Wang Z, Jensen LD, Hedlund EM, et al. PDGF-BB modulates hematopoiesis and tumor angiogenesis by inducing erythropoietin production in stromal cells. Nat Med. 2011;18:100–10.
8. McMaster WG, Kirabo A, Madhur MS, Harrison DG. Inflammation, immunity, and hypertensive end-organ damage. Circ Res. 2015;116:1022–33.
9. Hosaka K, Yang Y, Seki T, Nakamura M, Andersson P, Rouhi P, et al. Tumour PDGF-BB expression levels determine dual effects of anti-PDGF drugs on vascular remodelling and metastasis. Nat Commun. 2013;4:2129.
10. Hosaka K, Yang Y, Seki T, Du Q, Jing X, He X, et al. Therapeutic paradigm of dual targeting VEGF and PDGF for effectively treating FGF-2 off-target tumors. Nat Commun. 2020;11:3704.
11. Hosaka K, Yang Y, Seki T, Fischer C, Dubey O, Fredlund E, et al. Pericyte-fibroblast transition promotes tumor growth and metastasis. Proc Natl Acad Sci USA. 2016;113:E5618–27.
12. Hosaka K, Yang Y, Nakamura M, Andersson P, Yang X, Zhang Y, et al. Dual roles of endothelial FGF-2-FGFR1-PDGF-BB and perivascular FGF-2-FGFR2-PDGFRbeta signaling pathways in tumor vascular remodeling. Cell Disco. 2018;4:3.
13. Liu C, Zhang Y, Lim S, Hosaka K, Yang Y, Pavlova T, et al. A zebrafish model discovers a novel mechanism of stromal fibroblast-mediated cancer metastasis. Clin Cancer Res. 2017;23:4769–79.
14. Seki T, Hosaka K, Lim S, Fischer C, Honek J, Yang Y, et al. Endothelial PDGF-CC regulates angiogenesis-dependent thermogenesis in beige fat. Nat Commun. 2016;7:12152.
15. Brinkkoetter PT, Ising C, Benzing T. The role of the podocyte in albumin filtration. Nat Rev Nephrol. 2013;9:328–36.
16. Yang Y, Andersson P, Hosaka K, Zhang Y, Cao R, Iwamoto H, et al. The PDGF-BB-SOX7 axis-modulated IL-33 in pericytes and stromal cells promotes metastasis through tumour-associated macrophages. Nat Commun. 2016;7:11385.
17. Massagué J. TGFβ signalling in context. Nat Rev Mol Cell Biol. 2012;13:616–30.
18. Akhurst RJ, Hata A. Targeting the TGFβ signalling pathway in disease. Nat Rev Drug Disco. 2012;11:790–811.

19. Lamouille S, Xu J, Derynck R. Molecular mechanisms of epithelial-mesenchymal transition. Nat Rev Mol Cell Biol. 2014;15:178–96.
20. Piera-Velazquez S, Jimenez SA. Endothelial to mesenchymal transition: role in physiology and in the pathogenesis of human diseases. Physiol Rev. 2019;9:1281–324.
21. Cao Y. Multifarious functions of PDGFs and PDGFRs in tumor growth and metastasis. Trends Mol Med. 2013;19:460–73.
22. Schmierer B, Hill CS. TGFbeta-SMAD signal transduction: molecular specificity and functional flexibility. Nat Rev Mol Cell Biol. 2007;8:970–82.
23. Yang L, Inokuchi S, Roh YS, Song J, Loomba R, Park EJ, et al. Transforming growth factor-β signaling in hepatocytes promotes hepatic fibrosis and carcinogenesis in mice with hepatocyte-specific deletion of TAK1. Gastroenterology. 2013;144:1042–54.
24. Kang JS, Liu C, Derynck R. New regulatory mechanisms of TGF-beta receptor function. Trends Cell Biol. 2009;19:385–94.
25. Moustakas A, Heldin CH. Coordination of TGF-β signaling by ubiquitylation. Mol Cell. 2013;51:555–6.
26. Xia ZP, Sun L, Chen X, Pineda G, Jiang X, Adhikari A, et al. Direct activation of protein kinases by unanchored polyubiquitin chains. Nature. 2009;461:114–9.
27. Ozato K, Shin DM, Chang TH, Morse HC. TRIM family proteins and their emerging roles in innate immunity. Nat Rev Immunol. 2008;8:849–60.
28. Nisole S, Stoye JP, Saïb A. TRIM family proteins: retroviral restriction and antiviral defence. Nat Rev Microbiol. 2005;3:799–808.
29. Yan FJ, Zhang XJ, Wang WX, Ji YX, Wang PX, Yang Y, et al. The E3 ligase tripartite motif 8 targets TAK1 to promote insulin resistance and steatohepatitis. Hepatology. 2017;65:1492–511.
30. Hatakeyama S. TRIM family proteins: roles in autophagy, immunity, and carcinogenesis. Trends Biochem Sci. 2017;42:297–311.
31. Liu B, Zhang M, Chu H, Zhang H, Wu H, Song G, et al. The ubiquitin E3 ligase TRIM31 promotes aggregation and activation of the signaling adaptor MAVS through Lys63-linked polyubiquitination. Nat Immunol. 2017;18:214–24.
32. Song H, Liu B, Huai W, Yu Z, Wang W, Zhao J, et al. The E3 ubiquitin ligase TRIM31 attenuates NLRP3 inflammasome activation by promoting proteasomal degradation of NLRP3. Nat Commun. 2016;7:13727.
33. Cheng J, Xue F, Zhang M, Cheng C, Qiao L, Ma J, et al. TRIM31 deficiency is associated with impaired glucose metabolism and disrupted gut microbiota in mice. Front Physiol. 2018;9:24.
34. Ra EA, Lee TA, Won KS, Park A, Choi HJ, Jang I, et al. TRIM31 promotes Atg5/Atg7-independent autophagy in intestinal cells. Nat Commun. 2016;7:11726.
35. Yu C, Chen S, Guo Y, Sun C. Oncogenic TRIM31 confers gemcitabine resistance in pancreatic cancer via activating the NF-κB signaling pathway. Theranostics 2018;8:3224–36.
36. Blyszczuk P, Müller-Edenborn B, Valenta T, Osto E, Stellato M, Behnke S, et al. Transforming growth factor-β-dependent Wnt secretion controls myofibroblast formation and myocardial fibrosis progression in experimental autoimmune myocarditis. Eur Heart J. 2017;38:1413–25.
37. Pertel T, Hausmann S, Morger D, Züger S, Guerra J, Lascano J, et al. TRIM5 is an innate immune sensor for the retrovirus capsid lattice. Nature. 2011;472:361–5.
38. Tareen SU, Emerman M. Trim5 TAKes on pattern recognition. Cell Host Microbe. 2011;9:349–50.
39. Fan Y, Yu Y, Shi Y, Sun W, Xie M, Ge N, et al. Lysine 63-linked polyubiquitination of TAK1 at lysine 158 is required for tumor necrosis factor alpha- and interleukin-1beta-induced IKK/NF-kappaB and JNK/AP-1 activation. J Biol Chem. 2010;285:5347–60.
40. Ahmed N, Zeng M, Sinha I, Polin L, Wei WZ, Rathinam C, et al. The E3 ligase Itch and deubiquitinase Cyld act together to regulate Tak1 and inflammation. Nat Immunol. 2011;12:1176–83.
41. Fan Y, Shi Y, Liu S, Mao R, An L, Zhao Y, et al. Lys48-linked TAK1 polyubiquitination at lysine-72 downregulates TNFα-induced NF-κB activation via mediating TAK1 degradation. Cell Signal. 2012;24:1381–9.
42. Liang L, Fan Y, Cheng J, Cheng D, Zhao Y, Cao B, et al. TAK1 ubiquitination regulates doxorubicin-induced NF-κB activation. Cell Signal. 2013;25:247–54.
43. Guo J, Wang Z, Wu J, Liu M, Li M, Sun Y, et al. Endothelial Sirt6 is vital to prevent hypertension and associated cardiorenal injury through targeting Nkx3.2-GATA5 signaling. Circ Res. 2019;124:1448–61.
44. Whelton PK, Carey RM, Aronow WS, Casey DE, Collins KJ, Dennison HC, et al. 2017 ACC/AHA/AAPA/ABC/ACPM/AGS/APhA/ASH/ASPC/NMA/PCNA guideline for the prevention, detection, evaluation, and management of high blood pressure in adults: executive summary: a report of the American College of Cardiology/American Heart Association Task Force on Clinical Practice Guidelines. Circulation. 2018;138:e426–e483.
45. Sun X, He X, Zhang Y, Hosaka K, Andersson P, Wu J, et al. Inflammatory cell-derived CXCL3 promotes pancreatic cancer metastasis through a novel myofibroblast-hijacked cancer escape mechanism. Gut. 2021. gutjnl-2020-322744.
46. Lamb A, Chen J, Blanke SR, Chen LF. Helicobacter pylori activates NF-κB by inducing Ubc13-mediated ubiquitination of lysine 158 of TAK1. J Cell Biochem. 2013;114:2284–92.
47. Ji YX, Zhang P, Zhang XJ, Zhao YC, Deng KQ, Jiang X, et al. The ubiquitin E3 ligase TRAF6 exacerbates pathological cardiac hypertrophy via TAK1-dependent signalling. Nat Commun. 2016;7:11267.
48. Orning P, Weng D, Starheim K, Ratner D, Best Z, Lee B, et al. Pathogen blockade of TAK1 triggers caspase-8-dependent cleavage of gasdermin D and cell death. Science. 2018;362:1064–9.
49. Patrakka J, Tryggvason K. New insights into the role of podocytes in proteinuria. Nat Rev Nephrol. 2009;5:463–8.
50. Jiang X, Chen ZJ. The role of ubiquitylation in immune defence and pathogen evasion. Nat Rev Immunol. 2011;12:35–48.
51. Kawai T, Akira S. Regulation of innate immune signalling pathways by the tripartite motif (TRIM) family proteins. EMBO Mol Med. 2011;3:513–27.
52. Fan Y, Yu Y, Mao R, Zhang H, Yang J. TAK1 Lys-158 but not Lys-209 is required for IL-1β-induced Lys63-linked TAK1 polyubiquitination and IKK/NF-κB activation. Cell Signal. 2011;23:660–5.

ACKNOWLEDGEMENTS

We thank Dr. Yuan Zhang (Qilu Hospital of Shandong University, China) for the advice on the data analysis.

AUTHOR CONTRIBUTIONS

MZ, YZ, CG and CZ designed, supervised the study, and revision and final approval of the manuscript; JZ contributed to data research, analysis, and manuscript writing. LC, XW, QL, MZ, CC, LY, FX, WS, SS, NI, PB, FG, GS and BL contributed to data collection and analysis. J.Zhen acquired human samples. All the authors have read the manuscript and provided useful comments.

FUNDING INFORMATION

This work was supported by grants of the National Natural Science Foundation of China (Nos. 81970373, 31770977, 81770442, 31400771, 82030051 and 81920108003), the Program of Introducing Talents of Discipline to Universities (BP 0719033), the Postdoctoral Science Foundation of China and Shandong Province (Nos. 2018M630789 and 201901009), the Shandong Provincial Natural Science Foundation (ZR2020YQ53), the Taishan Scholars Program of Shandong Province (MZ and CZ), the Fundamental Research Funds for the Central Universities (No. 2018JC001), and the program for Outstanding PhD candidate of Shandong University (JZ).

COMPETING INTERESTS

The authors declare no competing interests.

ETHICAL STATEMENT

All mice experiments were carried on following the general guidelines published by the Association for Assessment and Accreditation of Laboratory Animal Care, approved by the Laboratory Animal Committee of Shandong University Qilu Hospital (Jinan, Shandong Province, China) (Permit number: DWLL-2017-018). In accordance with the principles of the Declaration of Helsinki, the investigations were approved by the Research Ethics Committee of Shandong University Qilu Hospital after informed consent was obtained from the patients (Permit number: KYLL-2017-605).

ADDITIONAL INFORMATION

Supplementary information The online version contains supplementary material available at https://doi.org/10.1038/s41418-021-00874-0.

Correspondence and requests for materials should be addressed to Chengjiang Gao, Meng Zhang or Yun Zhang.